PHYSICAL REVIEW B VOLUME 61, NUMBER 7 15 FEBRUARY 2000-I

Magnetic linear dichroism in angular-resolved Fe 3p and Fe 2p core-level photoemission for thin Fe films on graphite

S. H. Baker, K. W. Edmonds, A. M. Keen, S. C. Thornton, C. Norris, and C. Binns
Department of Physics and Astronomy, University of Leicester, University Road, Leicester LE1 7RH, United Kingdom

(Received 11 August 1999)

Magnetic linear dichroism in angle-resolved Fe 3p and Fe 2p core-level photoemission is used as a probe of the surface magnetism for thin Fe films with a range of surface morphologies. The Fe films were prepared by deposition in ultrahigh vacuum on to graphite substrates. Samples studied include an islanded film (mean diameter 100 nm), an array of ''wires'' (50–100-nm diameter) and a 150-nm-thick continuous film. The effect on the dichroism asymmetry of varying the magnitude of the magnetizing field, the film temperature and morphology is described. The data show an increased magnetic hardness and reduced magnetic transition temperature with decreasing dimension of the Fe features. A magnetic transition temperature of 720 K is measured for the islanded film while the continuous film shows essentially bulklike behavior. The development of magnetization in the films with increasing coverage is also studied. The results of fitting Zeeman-like multiplets to both Fe 3p and Fe 2p spectra are described.

INTRODUCTION

A variety of experimental techniques are available for use as probes of magnetism at surfaces and interfaces. Certain limitations associated with some of these, however, can restrict their usefulness. The magneto-optic Kerr effect, for example, is not surface sensitive, although it can be usefully applied to magnetic layers on nonmagnetic substrates.[1] Spin-resolved photoelectron spectroscopy of core levels and valence bands[2,3] offer direct probes of surface magnetism; however, they generally suffer from low efficiency of spin detection. An alternative to spin-resolved techniques is provided by dichroism experiments. Under certain conditions, changes in the lineshapes and/or intensities of core level absorption or photoemission spectra occur when the relative orientation of the sample magnetization is altered with respect to the polarization of the incident radiation; these changes can directly yield magnetic information on the ferromagnetic surface under study. The high fluxes of circularly and linearly polarized radiation required for dichroism experiments are readily available at synchrotron radiation sources.

Magnetic circular dichroism (MCD) experiments performed in x-ray absorption[4,5] are now well established. In such experiments, the spin and orbital magnetic moments of the incomplete valence shell can, with the aid of magnetooptical sum rules, be deduced from a comparison of the absorption cross-sections for different relative orientations of the radiation helicity and sample magnetization.[5–7] The first observations of dichroism using linearly polarized x-rays were made in absorption.[8] Subsequently, more attention has focused on magnetic linear dichroism (MLD) in photoemission.[9,10] Since photoemission experiments introduce a finite angular acceptance, the observed effects are more properly referred to as magnetic linear dichroism in the angular distribution (MLDAD) of photoelectrons. MLDAD provides information on magnetic exchange effects in core states.[11–13] The first experimental observations of MLDAD were by Roth *et al.*[9,14] and Rossi and coworkers[10,15] in Fe 3p core-level spectra measured off Fe (001) and (100) surfaces, respectively. The measured effects were large enough to indicate that MLDAD could be used as an *in situ* atom-specific magnetic probe for ferromagnetic surfaces.[16,17] With the help of spin-resolved data, measurements of MLDAD in Fe 3p core-level spectra [from Fe(001) on Ag(001) and Au(001)] showed that the effect can be attributed to the coexistence of spin-orbit and exchange-induced spin polarization in the spectra.[9] From measurements of MLDAD in Fe 3p spectra from Fe(100), Sirotti and Rossi[15] derived the fine structure of spin-orbit and exchange split sub-levels in the Fe 3p core level by using an atomic-like sextuplet fit. By calculating the intensities expected for each m_j sub-level on the basis of atomic photoionization theory, Rossi *et al.*[10] showed that a unique value of m_j could be assigned to each sub-level of the fitted sextuplet. The ordering between the two sub-levels in the spin-orbit split $J=\frac{1}{2}$ level was found to be reversed with respect to the anomalous Zeeman effect. Similar analysis has recently been extended to MLDAD measured from Fe 2p core-level spectra[18,19] and has helped to confirm the validity of the Zeeman-like approach referred to above.

In the present paper, MLDAD measurements on Fe samples with a range of surface morphologies are reported. MLDAD has been used to probe the magnetism in these samples as a function of magnetizing field and temperature. A multiplet fitting procedure similar to that referred to above has been applied to the spectra. Data for both Fe 3p and Fe 2p core levels are presented.

EXPERIMENT

The experiments were performed on the undulator beamline 5U.1 of the synchrotron radiation source (srs) at Daresbury Laboratory. Beamline 5U.1 provides a high flux of linearly p-polarized radiation (E vector in the plane of incidence); a 1200 lines/mm plane grating monochromator (platinum-coated CVD SiC on a graphite substrate) complemented by a spherical focussing mirror (platinum-coated

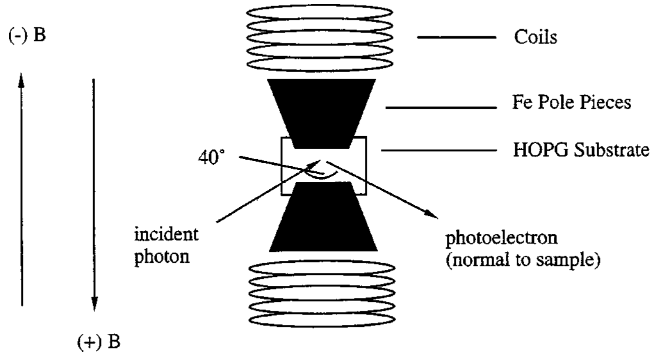

FIG. 1. Schematic illustration of the experimental geometry used in the MLDAD experiments.

fused silica) provides focused soft x-ray radiation over an energy range of approximately 50–1000 eV. Further details relating to the design of the undulator beamline may be found elsewhere.[20]

All measurements were carried out under ultrahigh vacuum (UHV) conditions, with a base pressure of 1×10^{-10} mbar or better. The Fe samples were prepared by evaporation from a water-cooled Knudsen source onto highly oriented pyrolytic graphite (HOPG) substrates; the pressure during evaporation was less than 3×10^{-10} mbar. A similar evaporation source could be used to overcoat Fe samples with an ultrathin Ag layer. The mosaicity in our samples was ±0.8°. Fresh HOPG surfaces were prepared by cleaving in air, prior to transferring to UHV. The graphite C(0001) surface is air stable and essentially inert to normal atmospheric constituents under ambient conditions. A small peak corresponding to the O 1*s* core level could occasionally be observed in the photoemission spectrum from freshly cleaved surfaces; modest heating to approximately 250 °C was normally sufficient to remove this feature. The HOPG samples were mounted on a liquid He-cooled cryostat.

A net magnetization was induced at the sample by pulsing a current through a copper coil whose axis was perpendicular to both the photon polarization and the emission direction of the photoelectrons. By using soft Fe pole pieces attached directly to the sample plate and pulsed currents up to 235 A, flux densities as high as 0.22 T could be generated. Figure 1 illustrates the experimental (chiral) geometry schematically. The photoelectrons were collected in normal emission by an H.A.100 analyser, while the incident *p*-polarized radiation impinged on the sample at an angle of 40° to the sample normal.

All data were collected in remanence. Fe $3p$ spectra were measured using a photon energy of 188 eV, with a combined monochromator/analyzer resolution of 0.25 eV, while the Fe $2p$ spectra were recorded at a photon energy of 850 eV, with a combined resolution of 0.55 eV.

Three Fe samples were studied in the present investigation:

(i) a thick continuous Fe film. Rutherford back scattering analysis on this film yielded a thickness of 15 nm.

(ii) an array of Fe ''wires,'' formed along steps in the HOPG substrate. Scanning electron microscope (SEM) images from a sample prepared under identical conditions (taken after removal from the experimental chamber) revealed that these wires were up to 10 μm in length and between 50 and 100 nm thick.

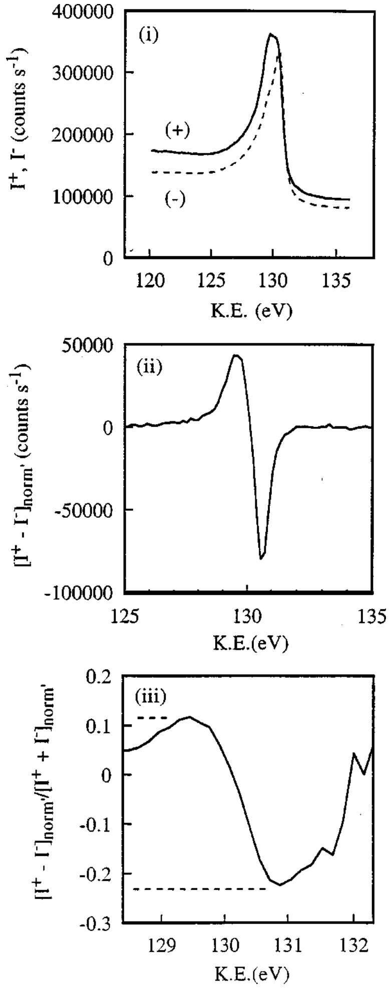

FIG. 2. Fe $3p$ spectra for the Fe wire sample recorded at room temperature and using a B field of 0.2 T. (i) Raw $3p$ spectra I^+ and I^-, at (+) and (−) magnetization, respectively. (ii) Difference (dichroism) spectrum $I^+ - I^-$ after background subtraction and normalization. (iii) Dichroism spectrum in (ii) divided by (background subtracted, normalized) sum $I^+ + I^-$.

(iii) a collection of Fe islands, formed by heating the wire sample to 550 °C. SEM analysis revealed that the mean size of the islands was 100 nm, with an (asymmetric) spread in sizes of 80–200 nm.

MLDAD IN FE 3*P* SPECTRA

Figure 2 illustrates the general dichroic features observed in the Fe $3p$ spectra for our samples, and the manner in which we have quantified the dichroism. Data for the Fe wire sample are presented, with the raw spectra for (+) and (−) magnetization given in Fig. 2(i). Initial observations indicate changes in lineshape upon field reversal which are qualitatively similar to those first observed by Roth *et al.*[9] and others.[10]

The smoothly varying background intensity in our spectra was fitted with a (power 6) polynomial plus a Tougaard contribution.[21] (This was carried out at the same time as peak fitting to the spectra, which is discussed later). Following background-subtraction and normalization to take account of

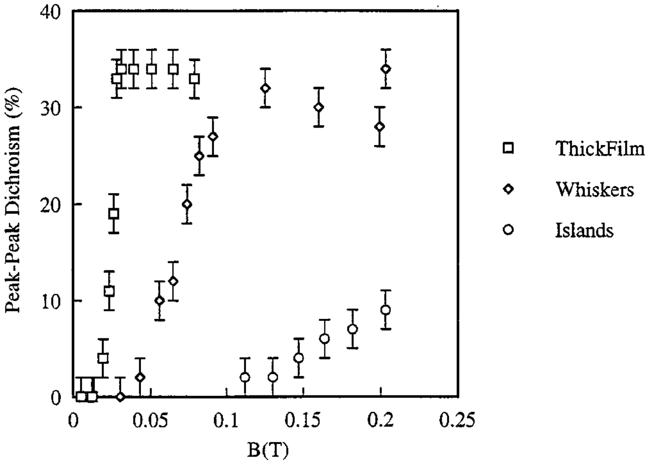

FIG. 3. Magnitude of dichroism signal (as defined in Fig. 2) as a function of applied magnetizing field *B*.

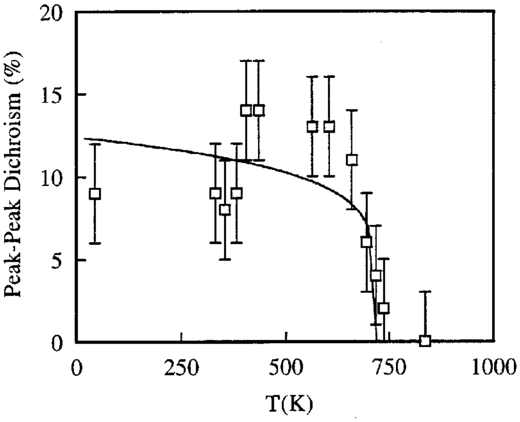

FIG. 4. Magnitude of dichroism signal as a function of temperature for the islanded sample. The full line represents the best fit to the data, according to Eq. (1).

beam current decay and any slight remanent magnetization effects in the chamber and analyzer, the dichroism spectra were obtained simply from the difference spectra, as illustrated in Fig. 2(ii). Dividing the dichroism spectrum by the sum of the normalized, background-subtracted spectra, as in Fig. 2(iii), gives the spectral dichroism as a percentage; the magnitude of the difference between the two peak values [approximately 34% in Fig. 2(iii)] provides a measure of the dichroism. The value of 34% in Fig. 2(iii) for the (saturated) Fe wire sample compares with a figure of 30% quoted by Roth *et al.*[14] for Fe (001) after background subtraction. In what follows, we have used the peak-to-peak values to quantify the dichroism in our samples.

THICK Fe FILM AND Fe WIRE SAMPLE

Figure 3 gives the strength of the dichroism signal in the Fe $3p$ core-level spectra as a function of applied magnetizing field B for the thick film and wire sample. The data were collected at room temperature. The thick film exhibits soft magnetic behavior, saturating for $B=0.03\,\mathrm{T}$. Further evidence of bulk-like behavior in this film comes from measurement of the MLDAD signal as a function of temperature. Performed over the temperature range 300–700 K, the data were satisfactorily fitted by means of the power law describing the temperature (T) dependence of magnetic ordering in a ferromagnet

$$\langle M\rangle \propto \{1-(T/T_C)\}^{\beta} \tag{1}$$

where $\langle M\rangle$ is the net magnetic moment, T_C is the Curie temperature, and β is the critical exponent that determines the rate at which magnetic ordering breaks down. Bulk (B) and surface (S) values of β have been measured previously for single crystal Fe using the magneto-optic Kerr effect and MLDAD, respectively,[17] and are given as $\beta_B=0.38\pm0.01$ and $\beta_S=0.81\pm0.01$. Data for the dichroism signal as a function of T in the thick Fe film yield a β value of 0.80 ± 0.02, using $T_C=1040\,\mathrm{K}$ (bulk value), hence confirming (as others have done[17]) the surface sensitivity of MLDAD.

The magnetically harder Fe wires require a B field of 0.1 T for saturation, the saturation value of the measured dichroism signal being approximately the same as for the thick film. It is also evident from Fig. 3 that they demonstrate appreciable coercivity. The length of the wires is sufficient to provide an easy axis of magnetization in the plane of the sample, which implies a uniaxial anisotropy rather than the cubic anisotropy of the bulk. As described earlier, the islanded sample was formed by heat treating the Fe wire sample; hence no MLDAD data are available for the latter as a function of temperature.

ISLANDED Fe SAMPLE

Also shown in Fig. 3 is the strength of the dichroism signal for the Fe islands as a function of B field. The measured dichroism is small compared to the saturation value in the other samples and measures only 9%, even at the maximum available B field. If the dichroism signal saturates at the same value as for the other two samples, i.e., ~34%, the field required for saturation can be estimated as 0.56 T by extrapolation of the data in Fig. 3. It should be pointed out, however, that the magnetization versus field curves when measured in remanence (as in this work) are more difficult to predict than for ''field-on'' measurements. In addition, the extrapolation procedure is not valid if the easy axis of magnetization is normal to the sample, in which case the in-plane remanence would be expected to be appreciably smaller than for the other two Fe samples. This would be consistent with the surface of the islands dominating the magnetic anisotropy of the sample. Observations of surface anisotropy in ultrathin Fe films on Au(111) (Ref. 22) indicate a decreasing in-plane remanence and increasing B field required for saturation as the film thickness is decreased. Overall, the data displayed in Fig. 3 show that the magnetic hardness of the Fe samples increases as their dimensionality is reduced.

Figure 4 shows the strength of the dichroism signal in the islanded sample, measured for an applied field $B=0.20\,\mathrm{T}$ as a function of temperature (over the range 40–850 K). The best fit to the data using Eq. (1) (also included in the figure) gives $\beta=0.16\pm0.02$ and $T_C=720\pm3\,\mathrm{K}$. The data in Fig. 4 represent a somewhat smoother transition to zero magnetization than that predicted by the fit. This may reflect the spread in island size (80–200 nm) in the sample, which would give rise to a range of Curie temperatures. The fit in Fig. 4 is therefore only considered as an average for the size range

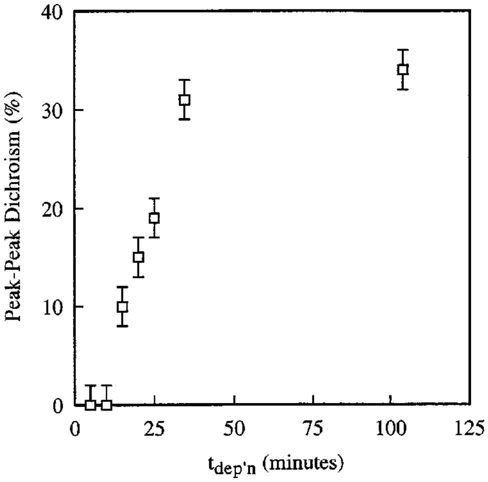

FIG. 5. Magnitude of dichroism as a function of growth time for an Fe sample grown at room temperature. The data points at 35 min and 104 min correspond to the Fe wire sample and the thick film, respectively.

present. Our results are still consistent, however, with predictions and observations that T_C and β are reduced in nanoscale systems. T_C has been observed to decrease with decreasing thickness in epitaxial Fe on Pd(100), with β values in the range 0.13–0.16;[23] submonolayer coverages yielded T_C values below room temperature. Similar results have been reported for epitaxial Fe on Au(100), for which β values of 0.21–0.22 (Ref. 24) were measured. The reduced transition temperature is a result of the reduced average atomic coordination due to the high proportion of surface atoms. (The modest increase in dichroism signal at ~400 K, evident in Fig. 4, may reflect a slight morphology change as the sample was heated. However, fits to the data with the 4 lowest temperature data points omitted yield the same value for T_C although with a somewhat enhanced value of β at 0.27).

After the MLDAD measurements as a function of field B and temperature T (see below) on the islanded Fe sample were completed, the sample was covered with an ultrathin ($\leqslant 1$ monolayer) coating of Ag at 40 K. After deposition of the Ag, no dichroism was observed even using the maximum available B field. The coating that this produces therefore results in a relative magnetic hardening or softening of this sample. A contributory factor to magnetic hardening in nanoscale systems is the enhanced orbital moment (m_0) observed in surfaces;[25] coating with another metal will reduce this. Alternatively, the extra strain induced by the overlayer could produce a hardening. A final possibility is that the easy axis of magnetization could have rotated from in-plane to out of plane.

DICHROISM AS A FUNCTION OF COVERAGE

Figure 5 shows the dichroism in an Fe sample (separate from those discussed above) as a function of coverage. The magnitude of the dichroism signal, measured at room temperature and with the maximum B field available of 0.2 T, is plotted as a function of deposition time. The C 1s core level, from the HOPG substrate, was also monitored with increasing coverage; a plot of the integrated C 1s intensity versus deposition time reveals a change in gradient at approximately 12 min, indicating a change in growth mode. No SEM images are available for this sample (at any coverage). However, from SEM images of the Fe samples discussed earlier (after removal from UHV), it is clear that the growth is not layer by layer. Instead, we suggest that the break point may correspond to a change from vertical columnar growth to lateral growth, as found for Mn islands on HOPG.[26]

The data in Fig. 5 are in qualitative agreement with the results discussed earlier, presented in Fig. 3, which confirm a correspondence of magnetic hardness on sample morphology. For the lowest coverages, where no remanent magnetization was measurable, the Fe islands may be small enough to act as a superparamagnetic array of single-domain particles. Above the blocking temperature of such an array, no dichroism signal would be expected. Blocking temperatures of 100–150 K have been observed for 10-nm Fe islands on MgO(001),[27] while 30 K has been reported for granular Fe in SiO_2.[28] At higher coverages, where the island sizes are above those for single-domain clusters to be favorable, the Curie temperature T_C is still expected to be less than for the bulk (as in the islanded sample discussed earlier). As the island size gradually increases with increasing deposition time, so does T_C; when the size becomes large enough that T_C is greater than room temperature, remanent magnetization is measured. After long-enough deposition times, continuous structures are eventually formed such as the wires or thick film discussed earlier.

MULTIPEAK FITS TO FE 3P SPECTRA

The multiplet fitting procedure, developed to model the fine structure in dichroic Fe 3p photoemission spectra,[10,15] was referred to earlier. The existence of such a fine structure is a consequence of the exchange interaction with the valence (3d) electrons, which lifts the degeneracy of the (spin-orbit split) core hole state into the various m_j sublevels (six in all for Fe 3p and Fe 2p-two for $j=1/2$, $[m_j=+1/2, -1/2]$ and four for $j=3/2$ $[m_j=+3/2,+1/2,-1/2,-3/2]$). In common with the work referred to previously,[10,15] we have applied atomiclike sextuplet fits to our Fe 3p spectra in an attempt to model the observed MLDAD changes as intensity changes in the various m_j sublevels upon field reversal.

Fits to the Fe 3p spectra in which the parameters for each of the six contributions are freely variable are clearly not justified. A constrained fitting procedure was therefore adopted. In order to help develop the fitting procedure, particularly with respect to locating at least some of the peak positions, two high-resolution Fe 3p spectra [at (+) and (−) maximum magnetization] were recorded for the Fe wire sample. The combined resolution ΔE for these spectra was 0.16 eV, attained by increasing the electron analyser resolution. Inspection of Fig. 6, which contains the spectra, shows that we have been at least partially successful in this respect. The (+) and (−) magnetization spectra were fitted simultaneously, using Doniach-Sunjic lineshapes and backgrounds consisting of a power six polynomial plus a Tougard contribution. Fits were optimised subject to the following general constraints: (i) the widths of the four $j=3/2$ sublevels were fixed to be equal (ii) the widths of the two $j=1/2$ sublevels were also fixed, with the lower KE component wider than the

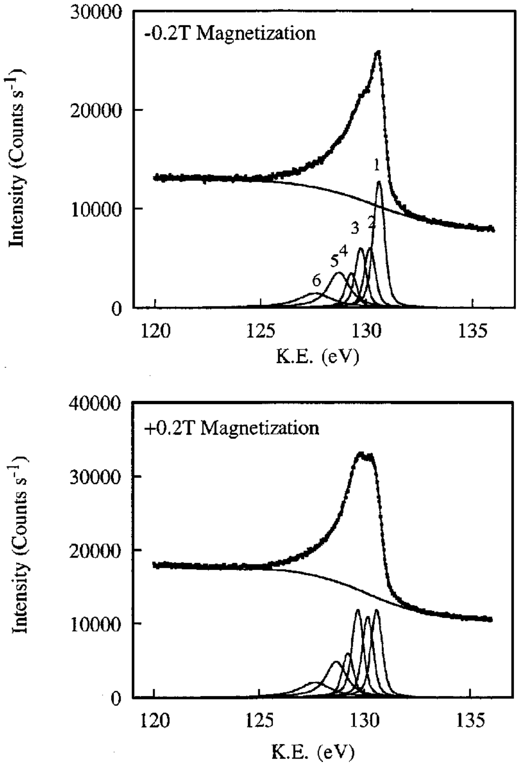

FIG. 6. High-resolution Fe 3p spectra for the Fe wire sample with associated sextuplet fits.

higher KE one (although fixing the two components to be equal did not significantly alter the fits) (iii) the asymmetries of all sub-levels were fixed to be equal. The results of the constrained sextuplet fits are shown in Fig. 6. Optimum fitted values for individual peak parameters are set out in Table I. In common with the results of Rossi *et al.*,[10] the separation between the two $j=1/2$ sublevels is larger than between adjacent $j=3/2$ sublevels. We also find that the fits required the Lorentzian widths of the two $j=1/2$ sublevels to be significantly greater than for the $j=3/2$ sublevels, although the $j=1/2$ sublevels are broader and the $j=3/2$ levels narrower than in the fits of Rossi *et al.*[10]

All other Fe 3p spectra were recorded at the normal (lower) resolution of 0.25 eV, quoted earlier, to allow reasonable data collection times. The remaining spectra for the wire sample were fitted using the parameters listed in Table I, with positions fixed to ±0.01 eV, leaving only the peak heights to be freely variable. In this way we were able to follow changes in the sextuplet fit results as a function of applied B field for the Fe wire sample. Of the six fitted contributions, peaks 1 and 3 show the largest changes on field reversal. There are clear changes in the relative intensities with increasing B, with the changes saturating above $B=0.1$ T as for the peak-to-peak data in Fig. 3. The changes in peaks 2 and 4 are much smaller while no significant changes in peaks 5 and 6 could be detected on field reversal for any value of B. It should be noted that for very low-B fields (where no changes were observed), the values for the fitted peak areas are (within error) the same as those deduced from the fit to an Fe 3p spectrum recorded for the Fe wire sample when unmagnetised.

It is interesting to compare in more detail our fitting results with those from elsewhere. From the fit parameters in Table I, the width of the $j=3/2$ multiplet between the $m_j=+3/2$ and $-3/2$ sublevels (a measure of the exchange splitting) is 1.3 eV, this leads to an average separation of 0.44 eV between the exchange split sublevels in the $j=3/2$ multiplet. The above values compare reasonably well with corresponding figures, taken from the data of Rossi and coworkers,[10] of 1.1 and 0.37 eV. Our results are also in fair agreement with theoretical work by Tamura *et al.*[13] who modelled Fe 3p soft x-ray photoemission spectra using a spin-polarized fully relativistic multiple scattering approach; by comparing their results with experimental data from Roth *et al.*,[9] the authors derived a value of 0.9–1.0 eV for the exchange splitting. Similarly, Hillebrecht *et al.*[29] used a splitting of 0.33 eV between adjacent $j=3/2$ sublevels when modelling Fe 3pMCD photoemission data. Our fitting results differ from some of those elsewhere in the identity of the sublevels showing the greatest intensity changes upon magnetization reversal. Peaks 1 and 3 (see Fig. 6) show the greatest intensity changes in our fits. In the fits of Rossi *et al.*,[10] peaks 1 and 4 (the $m_j=\pm 3/2$ levels) undergo the greatest changes. In addition, theoretical work by Cherepkov and Kuznetsov[30] and van der Laan[31] attribute the largest MLDAD changes in Fe 3p to the $m_j=\pm 3/2$ sublevels. As described earlier, the approach adopted in this work was to use the high resolution of the spectra in Fig. 6 to attempt to locate peak positions, rather than assigning peaks 1 and 4 to the points of maximum change in the MLDAD and then fitting the other sublevels accordingly. Indeed, applying the latter fitting approach to the spectra in Fig. 6 results in appreciably poorer

TABLE I. Optimum fit parameters derived from constrained sextuplet fits to Fe 3p spectra for Fe wire sample.

Positions of $j=3/2$ contributions	130.62±0.01 eV (Peak 1 $-$ $m_j=+3/2$)
	130.20±0.01 eV (Peak 2 $-$ $m_j=+1/2$)
	129.75±0.03 eV (Peak 3 $-$ $m_j=-1/2$)
	129.29±0.04 eV (Peak 4 $-$ $m_i=-3/2$)
Positions of $j=1/2$ contributions	128.72±0.02 eV (Peak 5 $-$ $m_j=-1/2$)
	127.67±0.04 eV (Peak 6 $-$ $m_j=+1/2$)
Widths of $j=3/2$ contributions	0.25±0.01 eV
Width of high K.E. $j=1/2$ contribution	0.95±0.05 eV
Width of low K.E. $j=1/2$ contribution	1.7±0.1 eV
Asymmetries	0.020±0.005

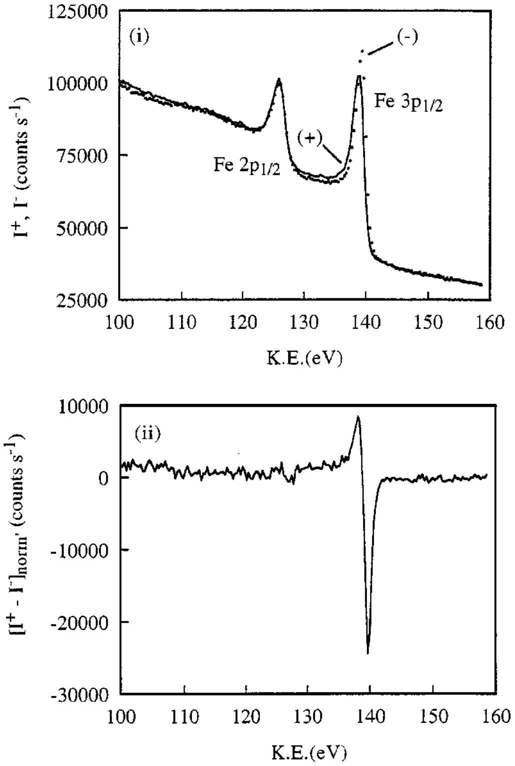

FIG. 7. Fe $2p$ spectra for the thick Fe film measured at room temperature and for an applied B field of 0.08 T. (i) raw spectra for (+) and (−) magnetization. (ii) difference spectrum after approximate normalization.

fits. The use of different lineshapes in the fitting analysis will result in slightly different peak positions. Contrary to analysis elsewhere[10] we have used Doniach-Sunjic line shapes, which we believe to be more accurate, in our fits; this could be responsible for the differences referred to above.

Sextuplet fits were also applied to the Fe $3p$ spectra recorded for the thick Fe film and islanded sample, as well as the Fe wire sample discussed above. Good fits for the thick film data were obtained using the same fit parameters as those in Table I. Similar changes in individual peak intensities to those described above are observed upon magnetization reversal. Any changes in peaks 5 and 6 are still too small to appear above the scatter in the data. In the case of the islanded sample, the spectra were shifted to slightly lower kinetic energy and broadened somewhat; lowering the fit positions of the peaks by 0.2 eV and broadening the widths of the $j=3/2$ contributions to 0.40 ± 0.01 eV yielded satisfactory fits to the data (with the fit parameters in Table I left otherwise unaltered). The only changes observable in the sextuplet fits with magnetization reversal are in peaks 1 and 3 for this sample. In each sample, the fitted sublevels, which show definite changes upon field reversal follow the same trends with varying field B or temperature T as the peak-to-peak dichroism. In order to detect any finer differences between the fit results of the various samples, high-resolution spectra for the thick film and islanded sample would be required.

MLDAD IN FE 2P SPECTRA

Fe $2p$ spectra for the thick Fe film were collected at room temperature for various magnitudes of magnetising field B.

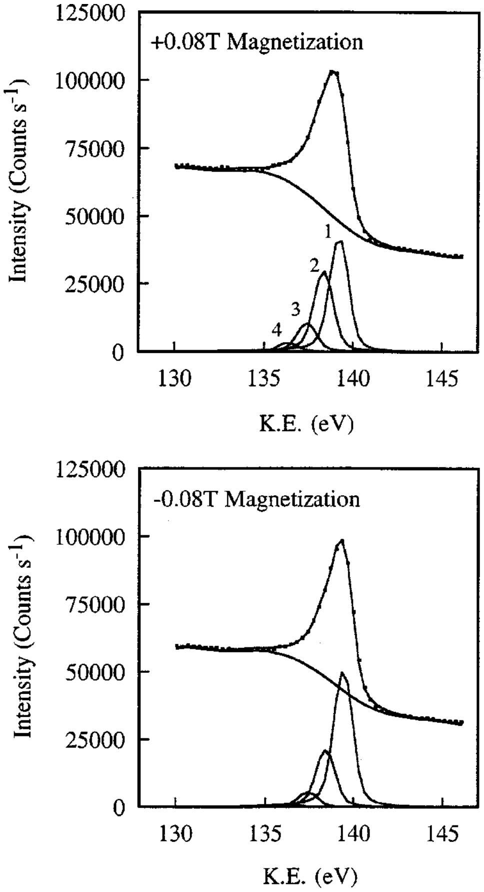

FIG. 8. Multiplet fits to Fe $2p_{3/2}$ for $B=\pm0.08$ T.

Figure 7(i) shows $2p$ spectra recorded after magnetization at fields of + and −0.08 T. The $2p_{3/2}$ and $2p_{3/2}$ levels are easily resolved on account of a large spin-orbit splitting of approximately 13 eV. The dichroism spectrum [(+) − (−)], obtained after approximately normalizing the two backgrounds to one another, is given in Fig. 7(ii). There is clear dichroism in the $2p_{3/2}$, with the same sign as was found in the $3p_{3/2}$, but little evidence for any observable dichroic effects in the $2p_{1/2}$, at least within the errors involved. This observation is consistent with our Fe $3p$ results. It, however, contrasts somewhat with the findings of Hillebrecht *et al.*[18] and Rossi *et al.*,[19] whose results show definite dichroism in the Fe $2p_{1/2}$ peak and of opposite sign to that seen in the Fe $2p_{3/2}$. Both groups of authors also observe a nonzero dichroic intensity, including small peaks, between the main features associated with the $2p_{3/2}$ and $2p_{1/2}$ peaks. As has been pointed out,[18,19] detailed analysis in this region is complicated by photoelectron diffraction effects and also the fact the spectral asymmetry values of weak features depend strongly on the background subtraction procedure adopted. In addition, discrete final-state configurations (satellites) may contribute to the dichroic intensity.[19]

As for the Fe $3p$ spectra, a constrained multi-peak fitting procedure has been used to model the $2p$ spectra, with two and four peak fits for the $j=1/2$ and 3/2 levels, respectively. In all cases, fits to the $j=1/2$ peaks yielded separations between the $m_j=+1/2$ and $-1/2$ contributions of 1.1 ± 0.1 eV. Similar energy spacings between the $j=3/2$ sublevels, of between 0.9 and 1.0 eV, are obtained in fits to the

$j=3/2$ peaks. Figure 8 shows four peak fits to the Fe $2p_{3/2}$ spectra for magnetizing fields of ± 0.08 T, for which the sample is saturated. As for the $3p$ analysis, peak positions were fixed to ± 0.01 eV and asymmetries to 0.025 ± 0.005. Optimum results were obtained with the widths of the $j=3/2$ sublevels at 0.40 ± 0.01 eV; the widths of the two $j=1/2$ sublevels were required to be broader (consistent with the $3p$ fit results), with the lower binding energy level at 0.80 ± 0.01 eV and the higher one at 1.4 ± 0.02 eV.

The above values for the exchange splitting between adjacent sublevels are approximately twice that found by Hillebrecht *et al.*[18] (0.5 eV) in their analysis of Fe $2p$ spectra from thin (>70 Å) Fe films on $W(110)$, and some four times the value calculated by Ebert *et al.*[32] of 0.27 eV. Rossi, Panaccione, and Sirotti[33] also deduce an appreciably smaller splitting of 0.35 eV in Fe(100). However, the sign of the intensity change in each of the sublevels upon magnetization reversal is the same as for the corresponding Fe $3p_{3/2}$ sublevels. We also find that the relative intensities and intensity changes on field reversal are similar to those given by Hillebrecht *et al.*[18] As for the peak-to-peak dichroism data in Fig. 3, the fitted results for the $2p_{3/2}$ multiplet are consistent with saturation for $B\geqslant 0.03$ T. From the lack of observable dichroism in the $j=1/2$ peak, we conclude not that it is absent in this level but that it is appreciably less than for the $j=3/2$. Certainly, others [18,19] have found the MLDAD signal in the $2p_{1/2}$ considerably reduced compared with that for the $2p_{3/2}$. Overall, the poorer resolution for the Fe $2p$ spectra compared to the $3p$ spectra requires the fit results for the $2p$ spectra to be treated with more caution than those for Fe $3p$.

SUMMARY

MLDAD has been used to probe the surface magnetism in Fe samples with a range of morphologies. The magnetic hardness of the Fe samples increases as their dimensionality is reduced. Consistent with results elsewhere,[23] the Curie temperature T_C and critical exponent β decrease as the dimension of the Fe features is reduced. T_C for the islanded film is 720 K, while the 150 nm film behaves essentially like bulk Fe. At very low-Fe coverages, no dichroism signal was measurable (at room temperature). However, above a certain coverage (at which point there is a change in growth mode), a dichroism signal is measurable which increases with increasing coverage. The Fe $3p$ spectra have been fitted successfully with Zeeman-like multiplets. Similar fits have been applied to the Fe $2p$ spectra.

---

[1] T. Beier, H. Jahrreiss, D. Pescia, Th. Woike, and W. Gudet, Phys. Rev. Lett. **61**, 1875 (1988).

[2] R. Allenspach, D. Mauri, M. Taborelli, and M. Landolt, Phys. Rev. B **35**, 4801 (1987).

[3] C. Carbone and E. Kisker, Solid State Commun. **65**, 1107 (1988).

[4] C. T. Chen, F. Sette, Y. Ma, and S. Modesti, Phys. Rev. B **42**, 7262 (1990).

[5] C. T. Chen, Y. U. Udzera, H-J. Lin, N. V. Smith, G. Meys, E. Chaban, G. H. Ho, E. Pellegrin, and F. Sette, Phys. Rev. Lett. **75**, 152 (1995).

[6] B. T. Thole, P. Carra, F. Sette, and G. van der Laan, Phys. Rev. Lett. **68**, 1943 (1992).

[7] P. Carra, B. T. Thole, M. Altarelli, and X. Wang, Phys. Rev. Lett. **70**, 694 (1993).

[8] G. van der Laan, B. T. Thole, G. A. Sawatsky, J. B. Goedkoop, J. C. Fuggle, J. M. Esteva, R. Karnatak, J. P. Remeika, and H. Dabkowska, Phys. Rev. Lett. **34**, 6529 (1986).

[9] Ch. Roth, F. U. Hillebrecht, H. B. Rose, and E. Kisker, Phys. Rev. Lett. **70**, 3479 (1993).

[10] G. Rossi, F. Sirotti, N. A. Cherepkov, F. Combet Farnoux, and G. Panaccione, Solid State Commun. **90**, 557 (1994).

[11] B. T. Thole and G. van der Laan, Phys. Rev. B **44**, 12 424 (1994).

[12] G. van der Laan, J. Magn. Magn. Mater. **148**, 53 (1995).

[13] E. Tamura, G. D. Waddill, J. G. Tobin, and P. A. Sterne, Phys. Rev. Lett. **73**, 1533 (1994).

[14] Ch. Roth, H. B. Rose, F. U. Hillebrecht, and E. Kisker, Solid State Commun. **86**, 647 (1993).

[15] F. Sirotti and G. Rossi, Phys. Rev. B **49**, 5682 (1994).

[16] G. Panaccione, F. Sirotti, and G. Rossi, J. Electron Spectrosc. Relat. Phenom. **76**, 189 (1985).

[17] F. Sirotti, G. Panaccione, and G. Rossi, Phys. Rev. B **52**, 17 063 (1995).

[18] F. U. Hillebrecht, Ch. Roth, H. B. Rose, W. G. Park, and E. Kisker, Phys. Rev. B **53**, 12 182 (1996).

[19] G. Rossi, G. Panaccione, F. Sirotti, S. Lizzit, A. Baraldi, and G. Paolucci, Phys. Rev. B **55**, 11 488 (1997).

[20] C. S. Mythen, G. van der Laan, and H. A. Padmore, Rev. Sci. Instrum. **63**, 1313 (1992).

[21] S. Tougaard, Phys. Rev. B **34**, 6779 (1986).

[22] G. Lugert and G. Bayreuther, Thin Solid Films **175**, 311 (1989).

[23] C. Liu and S. D. Bader, J. Appl. Phys. **67**, 5758 (1990).

[24] W. Dürr, M. Taborelli, O. Paul, R. Germar, W. Gudet, D. Pescia, and M. Landolt, Phys. Rev. Lett. **62**, 206 (1989).

[25] G. M. Pastor, J. Dorantes-Dávila, S. Pick, and H. Dreyssé, Phys. Rev. Lett. **75**, 326 (1995).

[26] C. Binns, S. H. Baker, A. M. Keen, S. N. Mozley, C. Norris, H. S. Derbyshire, and S. C. Bayliss, Phys. Rev. B **53**, 7451 (1996).

[27] Y. Park, S. Adenwalla, G. P. Felcher, and S. D. Bader, Phys. Rev. B **52**, 12 779 (1985).

[28] G. Xiao, S. H. Liou, A. Levy, J. N. Taylor, and C. L. Chien, Phys. Rev. B **34**, 7573 (1986).

[29] F. U. Hillebrecht, Ch. Roth, H. B. Rose, M. Finazzi, and L. Braicovich, Phys. Rev. B **51**, 9333 (1995).

[30] N. A. Cherepkov and V. V. Kuznetsov, J. Phys. B **22**, L405 (1989).

[31] G. van der Laan, J. Magn. Magn. Mater. **148**, 53 (1995).

[32] H. Ebert, L. Baumgarten, C. M. Scheider, and J. Kirschner, Phys. Rev. B **44**, 4406 (1991).

[33] G. Rossi, G. Pannaccione, and F. Sirotti, Phys. Rev. B **55**, 11 488 (1997).